

# Temperature insensitive long-period grating sensors in photonic crystal fibre

H. Dobb<sup>a</sup>, K. Kalli<sup>b</sup>, D.J. Webb<sup>a</sup>

<sup>a</sup> Photonics Research Group, Aston University, Aston Triangle, Birmingham, B4 7ET, UK.

<sup>b</sup> Higher Technical Institute, C. Kavafi Str., Aglantzia, P.O. Box 20423, 2152 Nicosia, Cyprus.

## ABSTRACT

Presented are long-period gratings (LPGs) fabricated in pure silica photonic crystal fibre (PCF) using an electric arc. Two different varieties of PCF have been investigated, an endlessly single mode PCF and a large-mode area PCF. The LPGs have been characterised for their sensitivity to a variety of external measurands. The LPGs in both fibres have been found to have negligible temperature sensitivity whilst exhibiting good sensitivity to bending and strain.

## 1. INTRODUCTION

A variety of diffracting structures can now be produced inside optical fibres, including Bragg gratings, long period gratings, chirped gratings, Moiré gratings,  $\pi$ -shifted gratings and blazed gratings. Many of these structures have properties which are dependent on the environment of the fibre and this has lead researchers to explore their potential as sensing devices. Although grating based sensing systems are at present a long way from being low cost, for certain applications they have a number of features which make them look attractive, such as their small size, dielectric nature, electrical passivity and large multiplexing capability.

The most mature of these technologies is the fibre Bragg grating and commercial systems have been available for a few years, with the price for an interrogation system recently falling below €10,000. However research into these devices continues and recently considerable effort has been devoted to the long period grating (LPG) [1]. In this paper we will compare the properties of the LPG with those of the FBG in order to justify our interest in these devices. We shall describe how the sensitivity of LPGs to various parameters is dependent on the fibre composition and geometry. We will then go on to present our latest work with LPGs written in photonic crystal fibre (PCF), where we have produced LPG sensors with negligible temperature sensitivities.

## 2. LPG PROPERTIES

A LPG consists of a periodic modulation of the waveguiding properties of a single mode optical fibre, typically on a scale of a few hundred microns. The modulation can take the form of a variation in the refractive index or geometry of the fibre and can be produced in a number of ways. Direct photoinscription is a popular approach and relies on the intrinsic sensitivity of some fibres to UV light [2]; photoinscription modifies the refractive index of the fibre core and is the preferred approach used to write FBGs. Because of the much larger period of LPGs in comparison with FBGs, it is also possible to produce these structures by modifying the fibre geometry using an electric arc [3], a CO<sub>2</sub> laser [4] or, for temporary devices, by applying a mechanical perturbation (microbending) [5].

The periodic modulation couples light from the core into a forward travelling cladding mode; these modes are quite heavily attenuated so that little of the coupled light will reach the far end of the fibre. Consequently, when illuminated by a suitable broadband source and viewed in transmission, the presence of an LPG is revealed by an attenuation band in the transmitted spectrum; in fact since coupling can occur to a series of cladding modes, there are usually a number of attenuation bands visible in the transmission spectrum.

Figure 1 shows the K-vector diagrams for diffraction from an LPG and an FBG. The former involves coupling to a cladding mode which has a similar propagation constant to the core mode; consequently the grating vector is much smaller than in the case of FBG diffraction where the coupling is between counter-propagating core modes. The much smaller grating vector in the case of the LPG translates into the much larger grating period required for these devices.

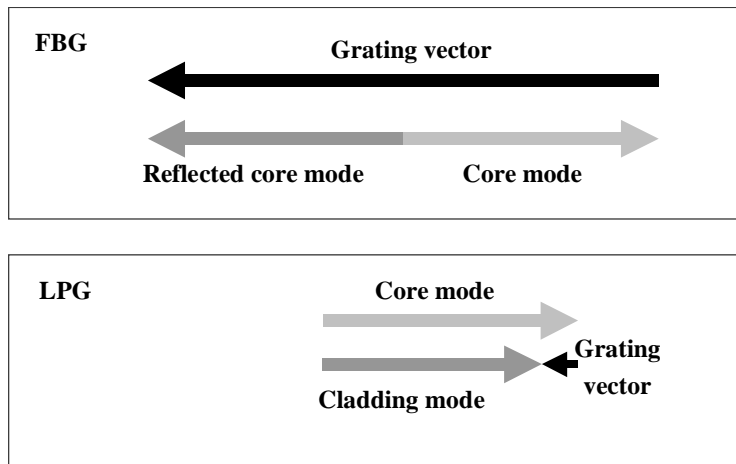


**Fig. 1.** K-vector diagram for diffraction from FBG (top) and LPG (Bottom).

The condition for resonant coupling between the core mode and a given cladding mode can be described by

$$\lambda_{res} = \Lambda(n_{core} - n_{cladd}) \tag{1}$$

where  $\lambda$  is the free space resonant wavelength,  $\Lambda$  is the grating period and  $n_{core}$  and  $n_{cladd}$  the effective indices of the relevant core and cladding modes, respectively. In general, the resonant wavelength is sensitive to strain, temperature, curvature and the index surrounding the cladding; these measurands may affect some or all of the terms on the RHS of equation 1.

### 3. COMPARISON OF LPGS and FBGS

LPG Disadvantages	LPG Advantages
Detected only in transmission	Ease of fabrication
Broader attenuation bands	Can have higher sensitivity
Complex spectra	Sensitivity to index/curvature
Sensitivity to more measurands	Multi-parameter sensing
	Dependence of sensitivity on core and cladding properties

**Table 1.** Advantages and disadvantages of LPGs in comparison with FBGs

The differences between FBGs and LPGs are summarised in Table 1. The size of the LPG period increases the number of techniques that can be used for fabrication, since producing the structure point-by-point is far easier than for FBGs. LPGs can only be detected in transmission, this reduces the options available when designing the optical system. LPGs tend to have a broader resonance, which will generally make the determination of the central wavelength less precise, though this is countered by the fact that LPGs can offer greater sensitivity to the various measurands than FBGs. Because there can be coupling to many cladding modes, LPGs have more complex spectra consisting of many attenuation bands; coupled with the larger attenuation bands and high sensitivity this may limit the number of devices that can be wavelength division multiplexed from a single source. On the positive side, the different attenuation bands

can have radically different sensitivities to the various measurands, thereby permitting two measurands to be recovered by monitoring two different bands from the same LPG. Unlike FBGs, LPGs can also be used to directly measure refractive index and curvature.

Last but definitely not least is the fact that the sensitivity of a given LPG attenuation band to a measurand is strongly dependent on the LPG period, the material properties of the core and cladding and the geometry of the fibre. By altering these parameters the sensitivity to a particular measurand can be varied considerably, both in magnitude and sign. Table 2 lists representative values that have been measured for FBGs and LPGs, both in conventional single mode fibre and also in fibres with other geometries, such as multiclad fibre or D-shaped fibre. It is this flexibility that we feel is the most important feature of LPGs and motivates our research. Ultimately, it should be possible to design a fibre to optimise the sensitivity to the desired measurand(s) whilst minimising, or removing completely, undesirable cross-sensitivities. As yet we have not met this goal, but we have investigated experimentally and theoretically the response of LPGs in a range of fibre types [6,7].

Feature	SMF telecoms optical fibre		LPGs in other fibre types	
	FBG	LPG	Maximum	Minimum
Period	0.5 $\mu\text{m}$	300 $\mu\text{m}$	-	-
Length	5 mm	5 cm	-	-
Width of attenuation bands	0.5 nm	8 nm	15 nm	3 nm
Number of attenuation bands	1 + harmonics	many	many	many
Temperature sensitivity @ 1550 nm	0.014 nm/ $^{\circ}\text{C}$	-0.41 nm/ $^{\circ}\text{C}$	+0.68 nm/ $^{\circ}\text{C}$	-0.56 nm/ $^{\circ}\text{C}$
Strain sensitivity @ 1550 nm	1.2 pm/ $\mu\epsilon$	+0.9 pm/ $\mu\epsilon$	+4.0 pm/ $\mu\epsilon$	-6.1 pm/ $\mu\epsilon$
Bend sensitivity @ 1550 nm	No	+9.5 nm.m	+9.5 nm.m	-7.4 nm.m
Index sensitivity @ 1550 nm	No	-465 nm	+5000 nm	-2400 nm

**Table 2.** Comparison of measurand sensitivities of FBGs and LPGs.

Recently we have extended this study from fibres with a more or less conventional core/cladding structure, to photonic crystal fibre (PCF). The motivation here is that the dispersion properties of PCF are strongly dependent on the microstructured geometry and it is possible to produce a wide variety of geometries using the usual stack-and-draw fabrication technique [8]; consequently we feel that PCF may offer an attractive route towards producing fibre that would enable LPG sensors to be optimised for specific applications.

#### 4. FABRICATION

LPGs are most commonly fabricated by exposing the optical fibre to UV laser radiation [2], either through an amplitude mask or by point-by-point inscription. In these fabrication techniques the fibre either has to be designed to be highly photosensitive or the fibre has to be slightly doped with germanium and hydrogen loaded to increase the photosensitivity and consequently the change in refractive index. If the fibre has been hydrogenated, post exposure thermal annealing needs to be undertaken to stabilise the gratings by removing the residual hydrogen. The electric arc technique does not require the fibre to be photosensitive or hydrogen loaded in order for LPGs to be fabricated. It has been shown by A. Malkli *et al.* [9] that the writing mechanism of the electric arc technique is to induce a small reduction in diameter and anisotropy in the fibre. This is a result of the regions of the fibre exposed to the arc experiencing densification of the glass structure. The anisotropy is likely to be due to the asymmetry of the electric arc discharge.

The LPGs in this paper were fabricated by exposing a stripped section of the PCF to the electric arc of a commercial splicer. The period of the LPG was controlled by applying the arc at set intervals, defined by a translation stage (TS), with the fibre under no tension, see Fig 2.

The characterisation of the attenuation bands was carried out by launching light from a broadband light source (BBS) into the fibre and monitoring the transmitted spectrum using an optical spectrum analyser (OSA), with an accuracy of 0.08nm. Two different types of PCF were investigated: endlessly single mode fibre from Blaze Photonics and large mode area fibre from Crystal Fiber.

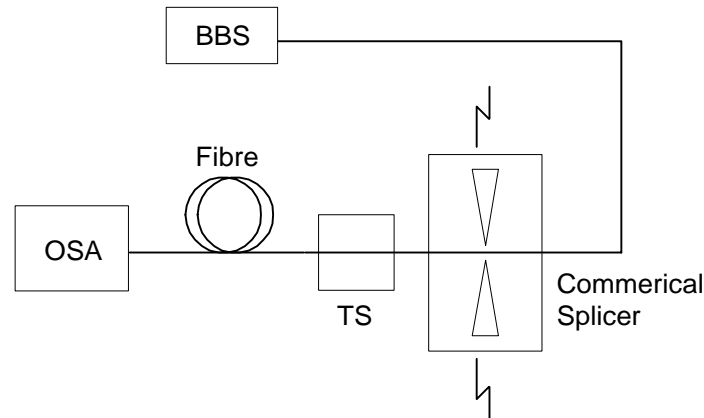


**Fig. 2.** Schematic of the electric arc fabrication technique.

## 5. ENDLESSLY SINGLEMODE PCF

In standard step index telecommunications fibre the number of guided modes in the core is determined by the V value

$$V = \left( \frac{2\pi a}{\lambda} \right) \left( n_{\text{core}}^2 - n_{\text{cladd}}^2 \right)^{1/2}, \quad (2)$$

where  $a$  is the core radius,  $n_{\text{core}}$  is the refractive index of the core and  $n_{\text{cladd}}$  is the refractive index of the cladding. The V number must be less than 2.405 for the fibre to be single mode. Consequently, ostensibly singlemode optical fibre can be multimode at lower wavelengths. Endlessly singlemode (ESM) PCF is designed to have singlemode operation for all wavelengths of light. The V number for PCF is approximated by [10],

$$V_{\text{eff}} = \left( \frac{2\pi\Lambda}{\lambda} \right) \left( n_{\text{no}}^2 - n_{\text{eff}}^2 \right)^{1/2}, \quad (3)$$

where  $\Lambda$  is the pitch (centre to centre spacing) of the holes,  $n_{\text{o}}$  is the refractive index of silica and  $n_{\text{eff}}$  is the effective cladding index based on the air hole fraction. The endlessly singlemode operation is achieved because at shorter wavelengths the light becomes more concentrated in the silica region of the fibre, avoiding the holes. This increases the effective cladding index, which counteracts the inverse relationship between the V number and the wavelength.

The particular ESM PCF used for this work (Blaze Photonics ESM-1550-01) had a core diameter of  $12\mu\text{m}$  surrounded by 54 air holes, with the space between adjacent holes being  $8\mu\text{m}$ , see Fig.3.



**Fig. 3.** Cross-section of the endlessly single mode PCF taken using a microscope with x 20 objective.

Several periods of LPG were fabricated, their transmission spectra being shown in Fig. 4. The location of LPG attenuation bands in standard telecommunications fibre e.g. SMF 28, increase in wavelength with an increase in grating period [11]. However, as can be seen in Fig 4, for the ESM PCF as the grating period increases the location of the attenuation bands decreases in wavelength. This is due to the effective refractive index of the cladding becoming lower at higher wavelengths due to the light intensity spreading into the air holes. From equation (1) it can be seen that this effect increases  $(n_{\text{core}} - n_{\text{cladd}})$  significantly with increasing wavelength, which results in the attenuation bands shifting to longer wavelengths for shorter grating periods [12].

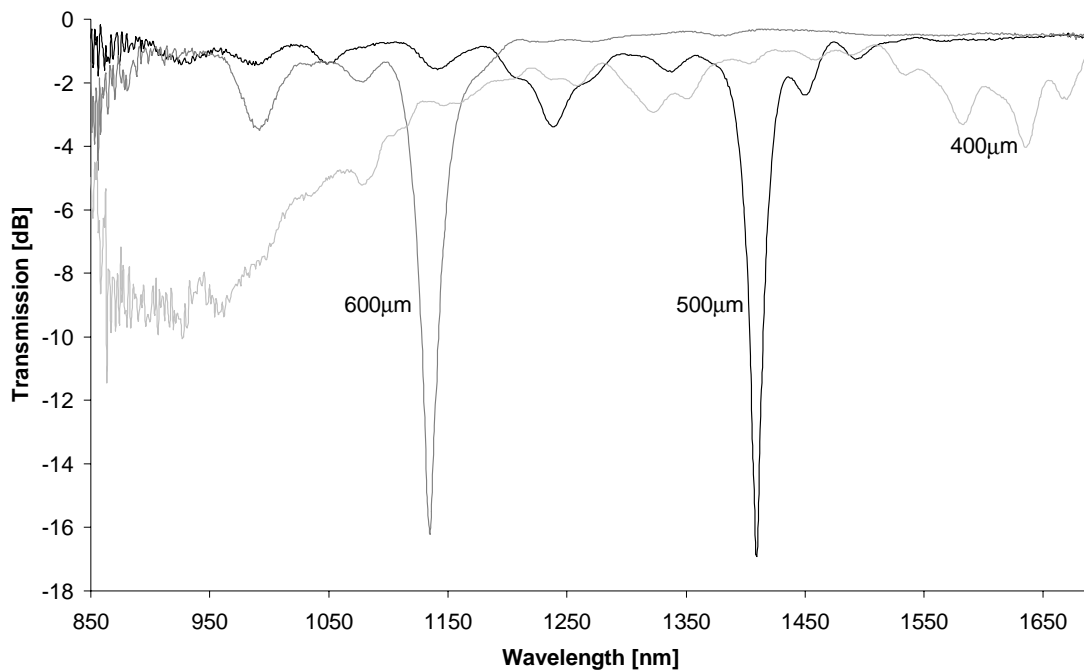


**Fig. 4.** Attenuation bands of different LPGs fabricated using the electric arc technique in ESM PCF. Dark Grey line 600µm; Black line 500µm; Light Grey line 400µm.

No significant attenuation bands are seen in the spectrum of the 400µm period LPG due to the attenuation bands being higher in wavelength than the optical range of the OSA. The 500µm period LPG, which had a length of 25.5mm, was

investigated for its spectral sensitivity to external measurands. Although a small band is seen at 1239nm, the 1409nm attenuation band was investigated due to this band being significantly stronger.

### 5.1 SPECTRAL TEMPERATURE CHARACTERISTICS OF ESM PCF

The temperature sensitivity was investigated by placing the LPG on an insulated Peltier heater. The temperature was varied from 20.0°C to 90.5°C, which produced no measurable change in the central wavelength of the attenuation band. From the measurement accuracy we have deduced a temperature sensitivity of  $d\lambda/dT=0 \pm 10 \text{ pm}/^\circ\text{C}$ . This may be compared with the results of Humbert et al. [13] who quote a temperature sensitivity of  $9 \text{ pm}/^\circ\text{C}$  in the range of 25-160°C for a similar structured PCF which varied from this PCF only by slightly differing core and hole dimensions. By way of further comparison, the temperature sensitivity of electric arc-induced LPGs in standard single mode fibre is  $70 \text{ pm}/^\circ\text{C}$  [14]. The difference between the fibre types occurs because standard single mode fibre has a germanium doped core which has a higher change in refractive index with temperature,  $dn/dT$ , than pure silica.

### 5.2 SPECTRAL BENDING CHARACTERISTICS OF ESM PCF

The bend sensitivity measurements were made by clamping the LPG midway between two blocks, one on a translation stage that was moved inwards, thereby bending the fibre; see Fig. 5.

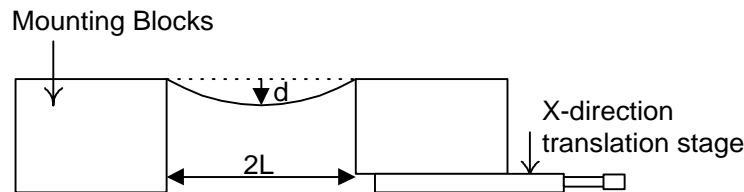
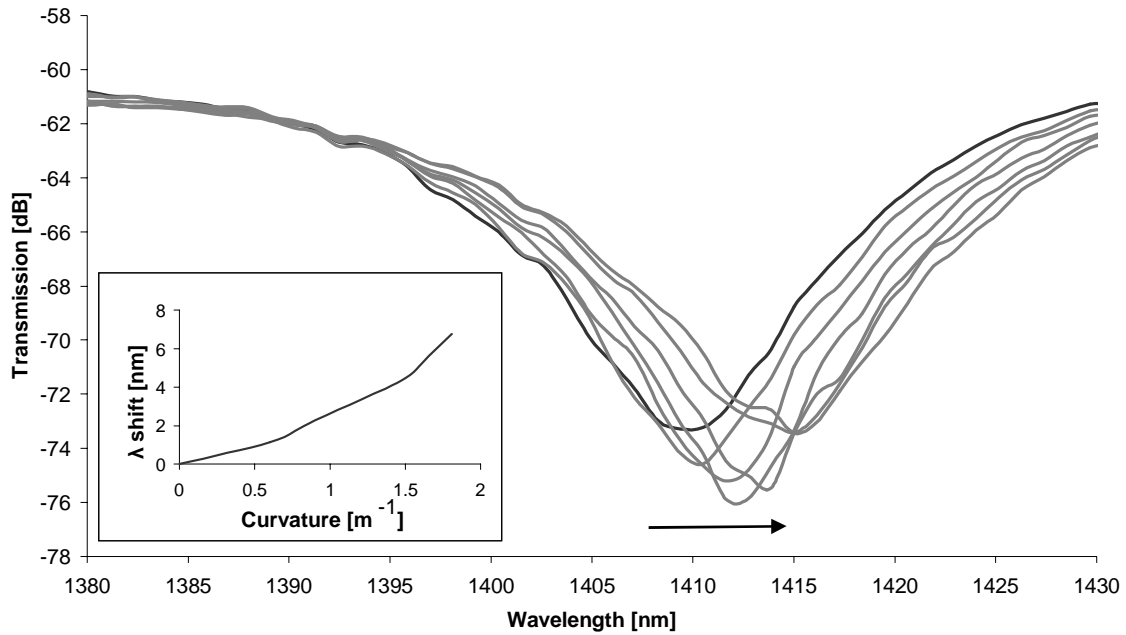


Fig. 5. Schematic of the bending rig.

When the LPG is midway between the two blocks, the resulting curvature,  $R$ , of the sensor is given by [15]

$$R = \frac{2d}{d^2 + L^2}, \tag{4}$$

where  $d$  is the bending displacement and  $L$  is half the distance between the fibre clamping points. The resulting change in the transmission spectrum is shown in Fig. 6.



**Fig. 6.** Spectral Response of 500  $\mu\text{m}$  LPG to curvature in range 0-1.81 $\text{m}^{-1}$   
 Bold curve corresponds to straight fibre. Inset: Wavelength shift as a result of induced curvature

With increasing curvature a red wavelength shift of the central wavelength was observed. The inset to Fig. 6 shows the relationship between the central wavelength shift and the curvature of the LPG; at a curvature of 1  $\text{m}^{-1}$  the bend sensitivity is  $d\lambda/dR=3.7 \pm 0.1 \text{ nm.m}$ .

### 5.3 SPECTRAL STRAIN CHARACTERISTICS OF ESM PCF

The strain sensitivity of the 1409 nm attenuation band was determined by fixing one end of the grating on a block and the other to a translation stage. The effect of the strain on the attenuation band is shown in Fig. 7. The resulting wavelength shift gives a strain sensitivity of  $d\lambda/d\sigma = -2.0 \pm 0.1 \text{ pm}/\mu\epsilon$ . The negative value of the sensitivity indicates a wavelength shift towards the blue with increasing strain. The shift of the attenuation band to lower wavelengths with applied strain is expected since the strain causes a temporary increase in the grating period. As previously shown, increasing the grating period in PCF causes the location of the LPG attenuation bands to shift to lower wavelengths.

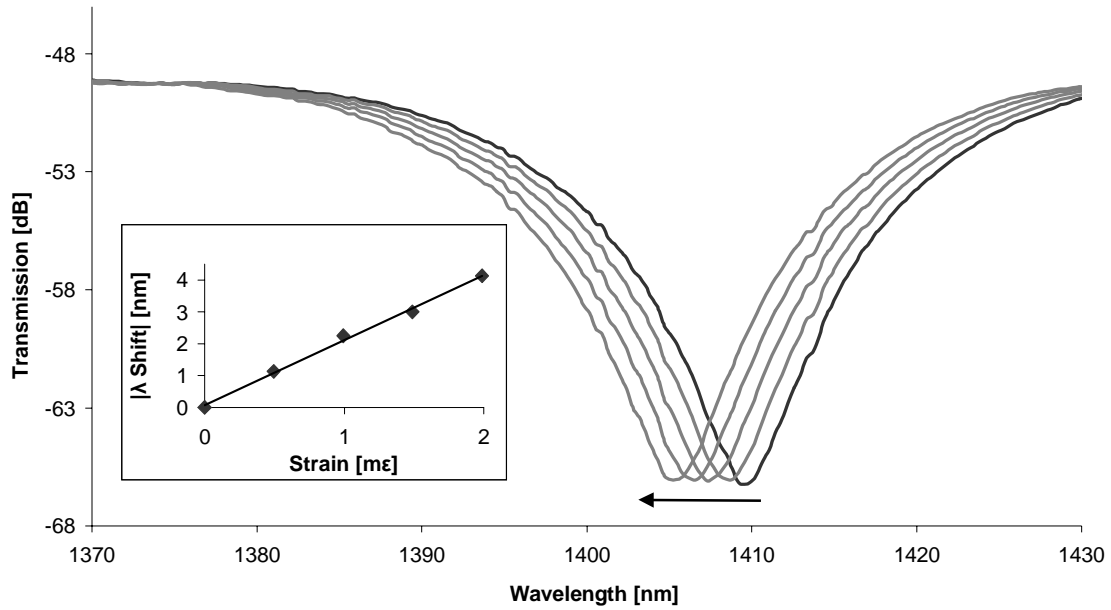


**Fig. 7** Spectral response of LPG to strain in range 0–1.98 mε  
 Unstrained curve in bold. Inset: Wavelength shift as a result of applied strain, showing straight line fit with  $d\lambda/d\sigma = -2.0 \pm 0.1 \text{ nm}/\mu\epsilon$ .

## 6 LARGE-MODE AREA PCF

The second PCF investigated was a Large-Mode Area (LMA) PCF (Crystal Fiber LMA 10). As with the previous fibre this too is designed to be endlessly single mode but with the difference that this fibre has a large effective mode field area, approximately  $40\mu\text{m}^2$ . This PCF had a core diameter of  $11\mu\text{m}$  and was surrounded by 90 air holes with a separation distance of  $7.1\mu\text{m}$ , see Fig. 8.

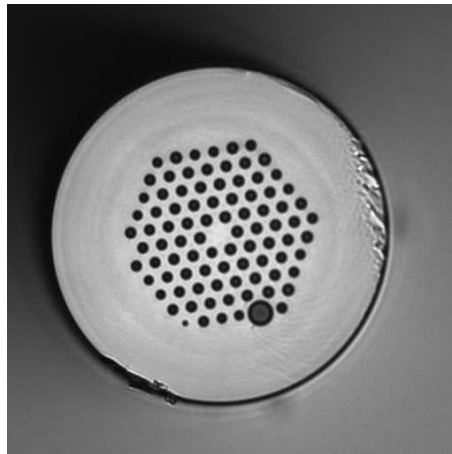


**Fig. 8.** Cross-section of the large-mode area PCF taken using a microscope with x 20 objective.

Once again several grating periods were fabricated (see Fig. 9) and as seen with the ESM PCF, increasing grating period decreased the location of the attenuation bands. Since the 600 $\mu\text{m}$  and 500 $\mu\text{m}$  LPGs did not have attenuation bands in a high enough wavelength range, the 400 $\mu\text{m}$  LPG was investigated for its sensitivity to external measurands.

The 400 $\mu\text{m}$  LPG had a length of 37.6mm and a transmission spectrum containing four attenuation bands located at 1668nm, 1511nm, 1434nm and 1389nm. These bands were investigated for their spectral sensitivity to external measurands.

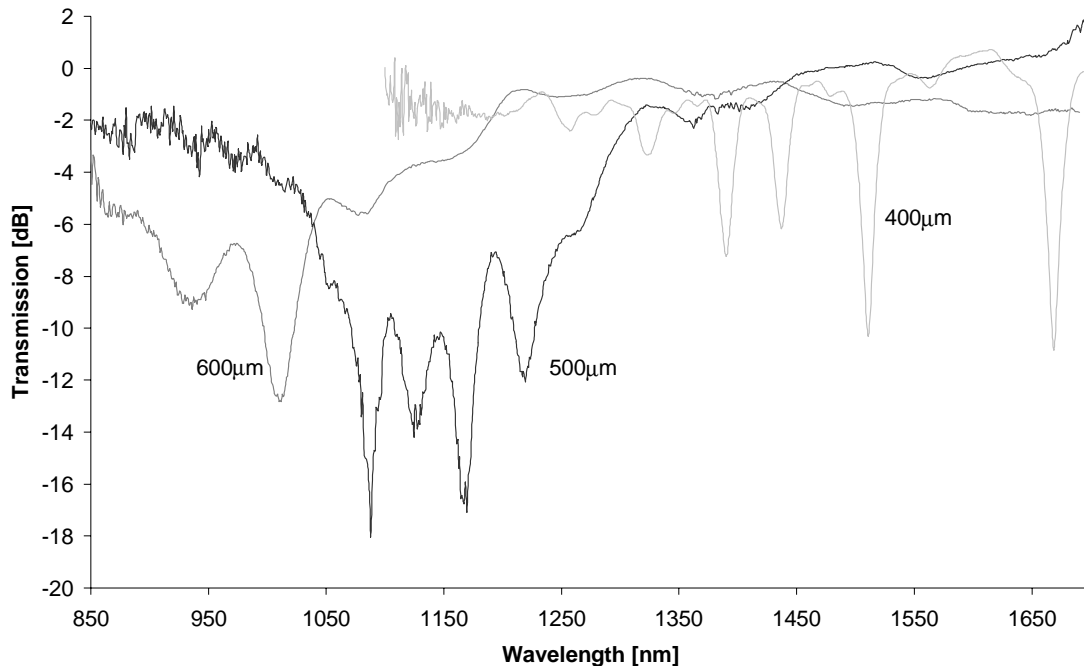


**Fig. 9.** Attenuation bands of different LPGs fabricated using the electric arc technique on LMA PCF. Dark Grey line 600 $\mu\text{m}$ ; Black line 500 $\mu\text{m}$ ; Light Grey line 400 $\mu\text{m}$ .

## 6.1 SPECTRAL TEMPERATURE CHARACTERISTICS OF LMA PCF

The temperature sensitivity was investigated again by placing the LPG on an insulated Peltier heater. The temperature was varied from 20.0°C to 90.2°C, which again produced no measurable change in the central wavelengths of any of the attenuation bands, from which we deduce a temperature sensitivity of  $d\lambda/dT=0 \pm 10 \text{ pm}/^\circ\text{C}$ .

## 6.2 SPECTRAL BENDING CHARACTERISTICS OF LMA PCF

The bend sensitivity was investigated using the same method as used with the previous PCF. However, in addition two rotational stages were fixed to the blocks and the fibre placed in the stages so that curvatures in different axes of the fibre could be investigated. The fibre was consequently bent with the rotational stages set at 0 degrees and the experiment repeated with the stages rotated by 180 degrees. This was done to investigate if the fibre had any directional curvature dependence.

The attenuation bands were found to be directionally sensitive with red and blue shifts in the central wavelength observed for the two orientations, see Fig. 10. With the rotational stages set at 0 degrees the attenuation bands at 1668nm and 1511nm experienced a blue wavelength shift while the bands at 1434nm and 1389nm experienced a red shift. With the rotational stages set at 180 degrees all shifts were in the opposite sense. It should be noted that the attenuation band at 1511nm experienced very small shifts and also decreased in amplitude.

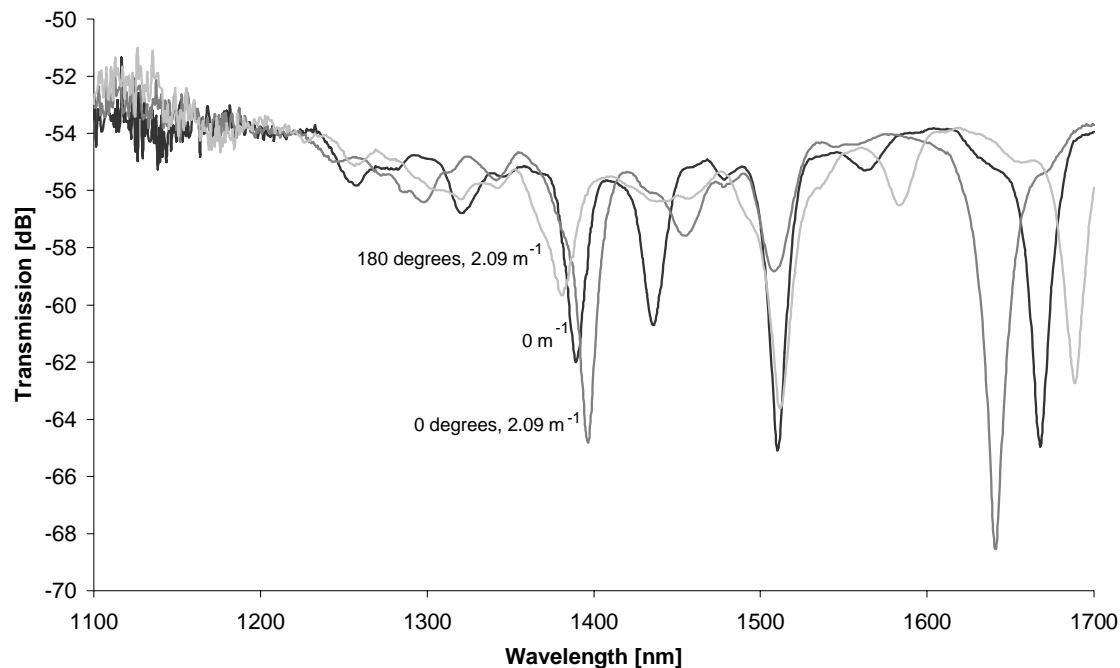


**Fig. 10.** Spectral response of the LPG to bending. Black line, LPG with no curvature; dark grey line, curvature of  $2.09\text{m}^{-1}$  in the 0 degrees position and light grey line curvature of  $2.09\text{m}^{-1}$  in the 180 degrees position.

The spectral sensitivity of all the attenuation bands was investigated and the band centred at 1668nm was found to have the maximum sensitivity to bending with a value of  $d\lambda/dR = 9.6 \pm 1.0 \text{ nm.m}$  with the fibre in the 180 deg rotational state and a sensitivity of  $d\lambda/dR = -12.4 \pm 1.2 \text{ nm.m}$  when in the 0 deg position; shown by the trend lines in Fig. 11.

The results for all the attenuation bands can be seen in Table 3. The negative signs indicate blue wavelength shifts.

	Atten. Band 1668nm	Atten. Band 1511nm	Atten. Band 1434nm	Atten. Band 1389nm
0 degree rotation	$-12.4 \pm 1.2 \text{ nm.m}$	$-1.1 \pm 0.1 \text{ nm.m}$	$6.5 \pm 0.3 \text{ nm.m}$	$4.5 \pm 0.4 \text{ nm.m}$
180 degree rotation	$9.6 \pm 1.0 \text{ nm.m}$	$0.7 \pm 0.1 \text{ nm.m}$	$-4.0 \pm 0.5 \text{ nm.m}$	$-4.3 \pm 0.5 \text{ nm.m}$

**Table 3.** Table showing the spectral responses of all the attenuation bands to the induced curvature

The spectral investigation of the band at 1668nm was taken up to a curvature of  $2.09\text{m}^{-1}$ , whereas the attenuation bands at 1511nm, 1434nm and 1389nm were taken up to  $1.45\text{m}^{-1}$ . This was because at larger curvatures it became increasingly difficult to determine the location of the bands at 1434nm and 1511nm due to their reduction in size. To the best of our knowledge these two rotational positions provide the maximum sensitivity to bending.

### 6.3 SPECTRAL SURROUNDING REFRACTIVE INDEX (SRI) CHARACTERISTICS OF LMA PCF

The spectral sensitivity to surrounding refractive index (SRI) was investigated by placing the LPG in a V-groove and immersing the grating in certified refractive index (CRI) liquids (supplied by Cargille laboratories Inc), which have a quoted accuracy of  $\pm 0.0002$ . Before immersion in each of the CRI liquids, to prevent contamination the LPG and V-groove were cleaned using methanol, then deionised water and finally dried.

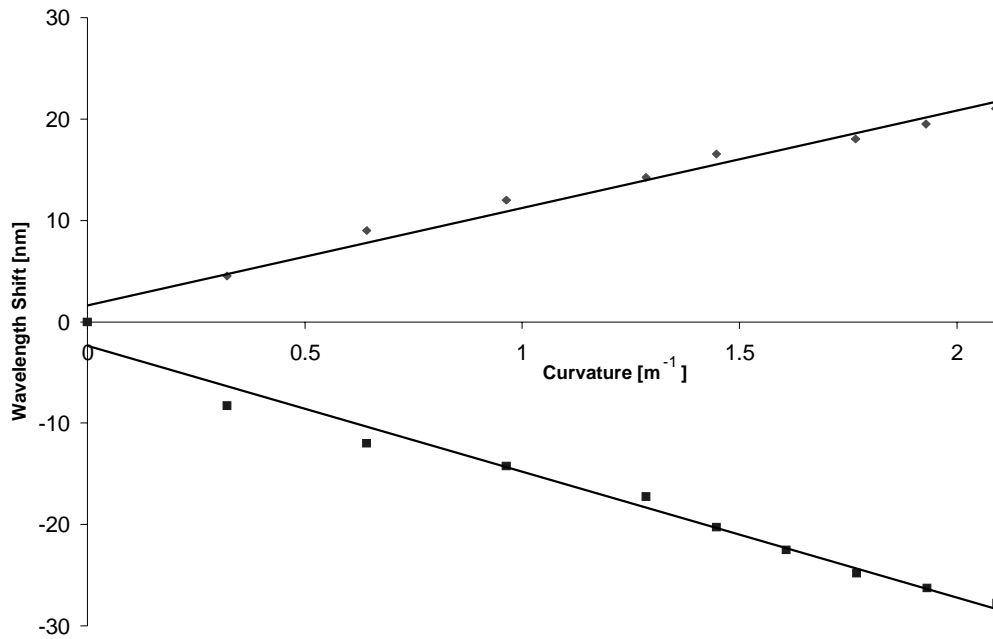


**Fig. 11.** Spectral sensitivity of the attenuation band at 1668nm to bending.

The V-groove was created in an aluminium plate, which had been machined flat to minimise the fibre bending. The plate was clamped to the optical table to ensure no movement. After each cleaning and subsequent repositioning of the fibre, it was ensured that the fibre was under the same tension each time by comparing the spectrum on the OSA with a saved trace of the original starting position. Several different CRI liquids were compared in the range  $n=1.325$  to  $n=1.514$ . Since the refractive index of silica is 1.47 this ensured the response of the grating to refractive indices lesser and greater than that of the fibre. Fig. 12 shows the effect of the SRI changes on the transmission spectrum of the grating with CRI liquids of index less than that of silica. As can be seen, all attenuation bands experience a red wavelength shift with increasing index.

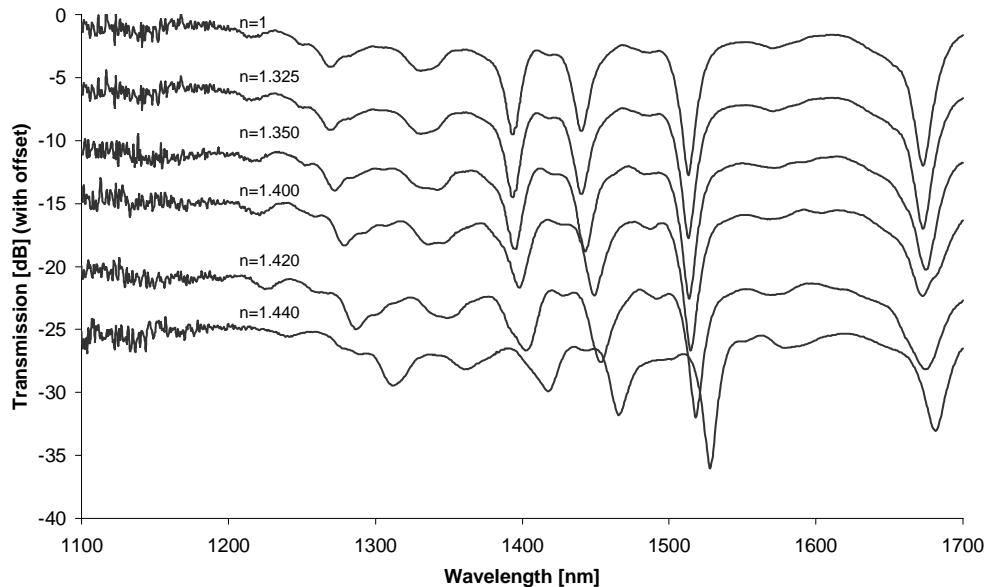


**Fig. 12.** The effect of SRI on the attenuation bands of the LPG.

The wavelength shift as a function of the SRI for each attenuation band is shown in Fig. 13. The figure shows that the peak initially centred at 1434nm has the greatest wavelength shift followed by the peak at 1389nm then 1511nm and finally 1668nm.

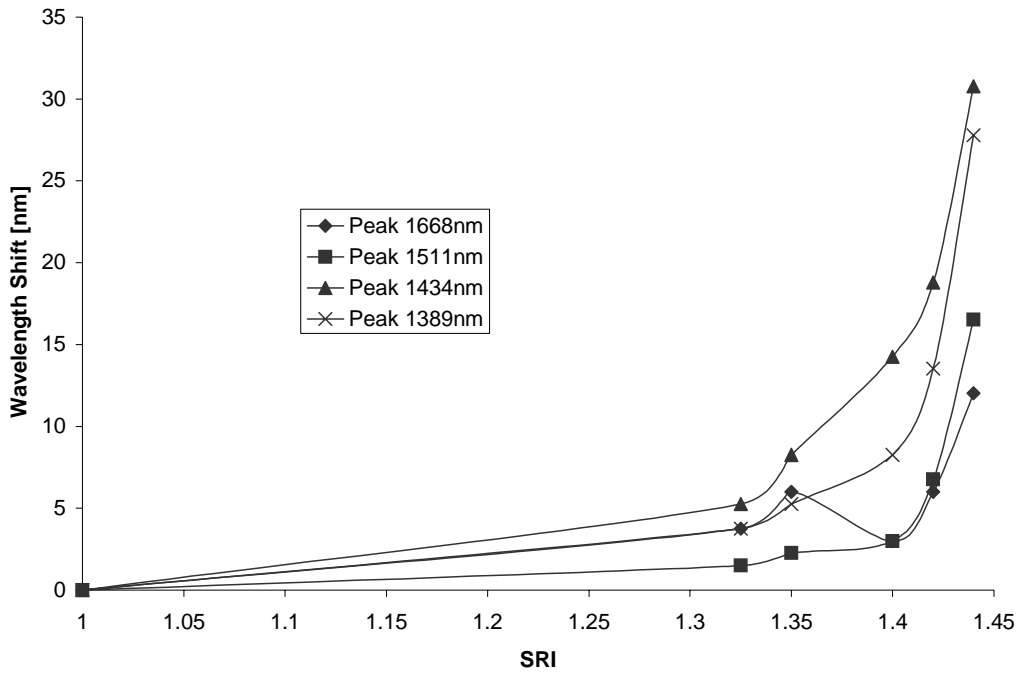


**Fig. 13.** The wavelength shift of the four attenuation bands as a function of the SRI (less than silica).

For refractive indices greater than that of silica, the spectrum of the LPG changes with only three attenuation bands present, see Fig. 14. This plot also shows that as the SRI is increased the amplitude of the attenuation bands grow and the fourth attenuation band starts to reappear.

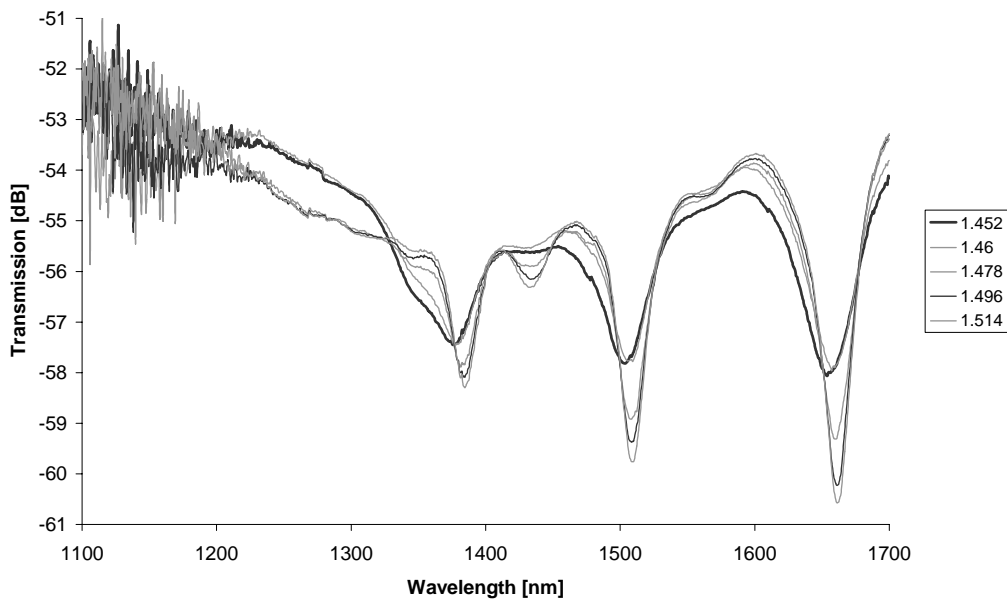


**Fig. 14.** The wavelength shift of the attenuation bands as a function of the SRI (greater than silica).

## 6.4 SPECTRAL STRAIN CHARACTERISTICS OF LMA PCF

The strain sensitivity of this LPG was investigated in the same way as the Blaze PCF. A linear blue wavelength shift of the central wavelength of all the attenuation bands was observed, see Fig. 15 for details of the band at 1668 nm. The attenuation band centred at 1668nm has a strain sensitivity of  $d\lambda/d\sigma = -2.5 \pm 0.04$  pm/ $\mu\epsilon$ . The other attenuation bands were also investigated and experienced roughly the same strain sensitivity, except for the band centred at 1389nm which had a sensitivity of  $d\lambda/d\sigma = -1.8 \pm 0.2$  pm/ $\mu\epsilon$ .

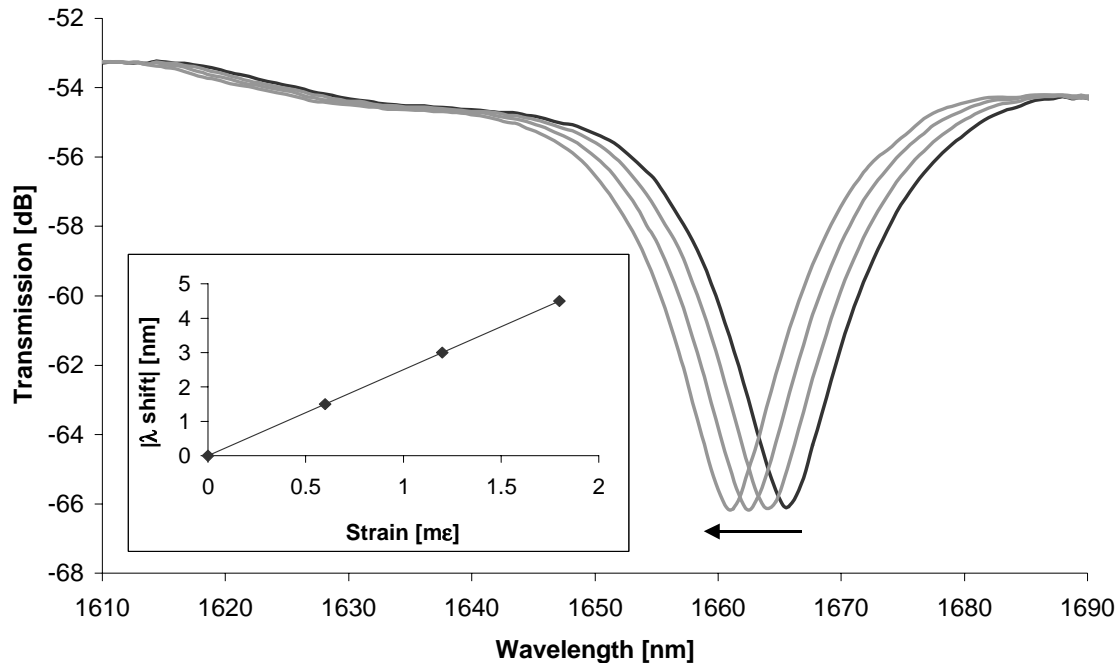


**Fig. 15.** Spectral response of LPG band at 1668 nm to strain in range 0–1.8m $\epsilon$ . Unstrained curve in bold. Inset: Wavelength shift as a result of applied strain

## 7 CONCLUSIONS

LPGs in two different types of PCF have been investigated. Both fibres have shown negligible temperature sensitivity whilst having significant sensitivity to other measurands. This is an important factor, since one of the persistent problems of using LPGs as sensors is their cross-sensitivity to temperature, which results in discriminatory schemes needing to be employed to separate the effect of temperature from the desired measurands. Since the electric-arc-induced LPGs studied here have been shown to possess attenuation bands with negligible temperature sensitivity, this eliminates the need for such schemes. Furthermore, since the fabrication process does not involve photoinscription, photosensitive fibre is not required and the cost of the resulting sensing system has the potential to be significantly reduced, as does the fabrication time itself.

The LPG fabricated in the Crystal Fiber PCF was found to have a maximum strain sensitivity of  $d\lambda/d\sigma = -2.5 \pm 0.04$  pm/ $\mu\epsilon$ , which is comparable to the Blaze Photonics PCF, which had a strain sensitivity of  $d\lambda/d\sigma = -2.0 \pm 0.1$  pm/ $\mu\epsilon$ . Both fibres were found to have a similar damage threshold breaking after a strain of 1.98 m $\epsilon$  for the Blaze Photonics PCF compared to after a strain of 1.8 m $\epsilon$  for the Crystal Fiber PCF. The Crystal Fiber PCF was also found to have a greater sensitivity to bending with its maximum sensitivity being  $d\lambda/dR = -12.4 \pm 1.2$  nm.m compared to  $d\lambda/dR = 3.7 \pm 0.1$  nm.m. The LPG in the Crystal Fiber PCF was also found to have directional bending properties.

## 8 REFERENCES

1. S.W. James and R.P. Tatam. 'Optical fibre long-period grating sensors: characteristics and application'. *Meas. Sci. Technol.*, 2003 **14** (5) pp R49-61
2. A.M. Vengsarkar, P.J. Lemaire, J.B. Judkins, V. Bhatia, T. Erdogan and J.E. Sipe. 'Long-period fiber gratings as band rejection filters'. *J. Lightwave Technol.*, 1996, **14**, pp. 58-64
3. G. Rego O. Okhotnikov, E. Dianov and V. Sulimov. 'High-temperature stability of long-period gratings produced using an electric arc'. *J. Lightwave Technol.*, 2001, **19**, (10) pp. 1574-1579
4. D.D. Davies T.K. Gaylord, E.N. Glytsis, S.G. Kosinski, S.C. Mettler and A.M. Vengsarkar. 'Long-period fibre grating fabrication with focused CO<sub>2</sub> laser pulses'. *Electron. Lett.*, 1998 **34** (3) pp. 302-303
5. J.W. Berthold III. 'Historical review of microbend fiber-optic sensors'. *J. Lightwave Technol.*, 1995, **13**, (7) pp. 1193-1199
6. T. Allsop, D.J. Webb and I. Bennion. 'A comparison of the sensing characteristics of long period gratings written in three different types of fiber'. *Opt. Fiber Tech.* 2003 (9), pp.210-223
7. T. Allsop, A. Gillooly, V.K. Mezentsev, T. Earthgrowl-Gould, R. Neal, D.J. Webb and I. Bennion. 'The Spectral Characteristics of Long Period Gratings Written in D-Shaped Optical Fiber as Bending Sensors'. *Proceedings of the 16th International Conference on Optical Fibre Sensors (OFS '2003)*, IEICE, Japan, 2003. pp. 88-91
8. J.C. Knight, T.A. Birks, P.St.J. Russell and D.M. Atkin. 'All-silica single-mode optical fiber with photonic crystal cladding'. *Opt. Lett.*, 1996, **21**, (19) pp. 1547-1549
9. A. Malki, G. Humbert, Y. Ouerdane, A. Boukhenter and A. Boudrioua. 'Investigation of the writing mechanism of electric-arc-induced long-period fiber gratings'. *Appl. Opt.*, 2003, **42**, (19) pp. 3776-3779
10. T.A. Birks, J.C. Knight and P.St.J Russell. 'Endlessly single-mode photonic crystal fiber'. *Opt. Lett.*, 1997, **22**, (13) pp. 961-963
11. X. Shu, L. Zhang and I. Bennion. 'Sensitivity Characteristics of Long Period Fiber Gratings'. *J. Lightwave Technol.*, 2002, **20**, pp 255-266
12. K. Morishita and Y. Miyake. 'Fabrication and resonance wavelength of long-period gratings in a pure-silica photonic crystal fiber by the glass structure change'. *J. Lightwave Technol.*, 2004, **22**,(2) pp. 625-630
13. G. Humbert, A. Malki, S. Février, P. Roy and D. Pagnoux. 'Electric arc-induced long-period gratings in Ge-free air-silica microstructure fibres'. *Electron. Lett.*, 2003 **39** (4) pp. 349-350
14. G. Humbert and A. Malki. 'Electric-arc-induced gratings in non-hydrogenated fibres: fabrication and high-temperature characterisations'. *J. Opt. A, Pure Appl. Opt.*, 2002, **4**, pp. 194-198
15. W. Du, H. Tam, M Liu and X. Tao. 'Long-period fiber grating bending sensors in laminated composite structure'. SPIE Conf. Proc. Smart Structures and Materials, SPIE, San Diego, USA, 1998, Vol.3330, pp. 284-292